Molecular Switches

DOI: 10.1002/ange.200600925

Electrical Conformational Bistability of Dimesogen Molecules with a Molecular Chord Structure**

Yan-Lian Yang, Qi-Lin Chan, Xiao-Jing Ma, Ke Deng, Yong-Tao Shen, Xi-Zeng Feng, and Chen Wang**

The design of molecular structures that can respond effectively to external conditions such as an electric field is a topic of continued interest. Electrically induced conformational changes at the single-molecule level were demonstrated by Qiu et al.[1] They observed reversible transitions between the planar and nonplanar conformational states of the porphyrin macrocycle as a result of structural flexibility. It has also been reported that controlled conformational changes can be achieved in the case of self-assembled monolayers (SAMs) with low-density functional groups.[2] Yet, it has been challenging to obtain conformational switching in densely packed SAMs by using an electric field because of strong intermolecular interactions. Herein, we demonstrate that conformational changes induced by an electric field can be achieved in densely packed SAMs consisting of dimesogen molecules with a soft linker unit, which gives rise to new alternatives in designing field-responsive molecular interfaces.

The category of dimesogen molecules contains molecular structures with two mesogenic units connected by a linker unit.[3] A number of studies have revealed that the rigidity of the linker unit could significantly affect the properties of symmetric cholesteric liquid crystals (ChLCs). As an example, dicholesteryl esters containing a diacetylene unit as a rigid linker in the flexible chain showed slower crystallization and formed a cholesteric solid by cooling from the cholesteric temperature to 0 °C.[4] These studies suggested that the rigidity of the linker and the intermolecular interactions are very important for the thermal and optical properties of dimesogen ChLCs, which are widely applied in molecular photonics or information technology, such as e-paper, commercial billboards, and power-saving liquid crystal displays.[3,5,6]

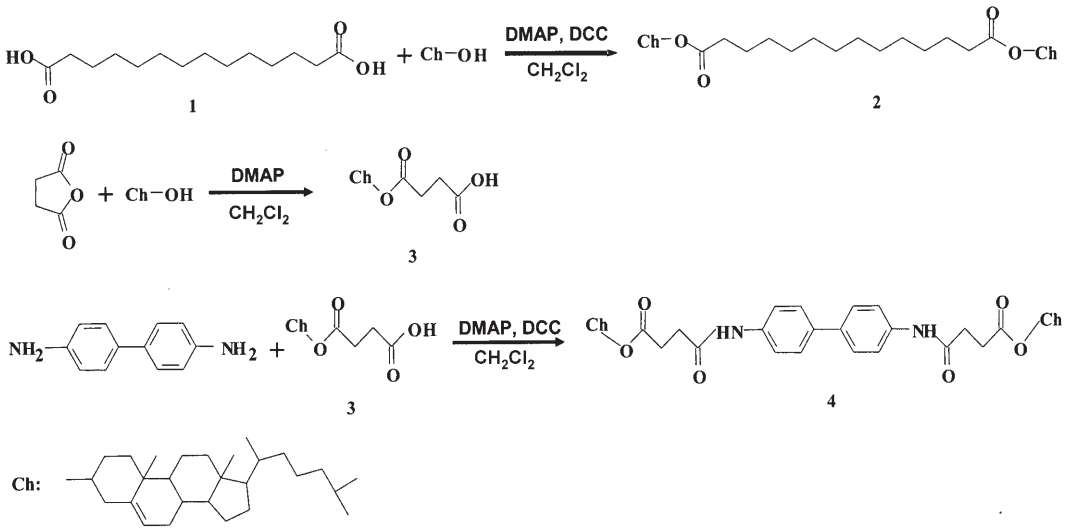

Scheme 1. Synthesis of cholesteryl esters Ch-14 (**2**) and CBC (**4**). DMAP = 4-dimethylaminopyridine, DCC = dicyclohexylcarbodiimide.

The submolecular resolution capability of scanning tunneling microscopy (STM) makes it possible to investigate the molecular arrangements in the self-assembled structures. Furthermore, the capability of STM measurement at different bias polarities allows in situ investigation of the electric field effects on the molecular assemblies. In this work, we designed and synthesized two kinds of low-molecular-weight compounds of cholesterol mesogens to explore the effects of the rigidity of the linker unit on the response to an electric field by using STM. As illustrated in Scheme 1, dicholesteryl tetradecanedioate (Ch-14, **2**; the linking unit is referred to as C_{14}) and 4,4′-([1,1′-biphenyl]-4,4′-diyldiimido)dibutanoic acid, bis(4-oxo-dicholesteryl ester) (CBC, **4**) were both synthesized

[*] Dr. Y. L. Yang, X. J. Ma, Dr. K. Deng, Prof. Dr. C. Wang
National Center for Nanoscience and Technology
Beijing 100080 (P.R. China)
Fax: (+86) 10-6256-2871
E-mail: wangch@nanoctr.cn
Q. L. Chan, Y. T. Shen, Prof. Dr. X. Z. Feng
College of Life Science
Nankai University
Tianjin 300071 (P.R. China)
Fax: (+86) 10-2350-7022
E-mail: xzfeng@nankai.edu.cn

[**] This work was supported by the National Natural Science Foundation of China (grant nos. 20473097, 90403140, 90406019, and 90406024) and the Tianjin Science Technology Research Funds of China (no. TJ043801111). Y.L.Y. acknowledges support from the State Key Laboratories of Transducer Technology.

Supporting information for this article is available on the WWW under http://www.angewandte.org or from the author.

through condensation reactions using DCC as the condensation reagent (see Supporting Information for detailed characterizations of the two compounds). The Ch-14 molecules contain two cholesterol mesogens linked by a flexible alkyl chain. The other specimen of CBC contains two mesogens connected by a rigid linker, biphenylene.

The molecular assembly structures of Ch-14 and CBC were studied by STM. Stripe-patterned images with a head-to-head configuration were observed for both types of molecules with slightly different assembly arrangements. More interestingly, when the bias polarity was switched during imaging, drastic changes in the molecular image were observed for Ch-14, while no discernible changes could be observed for CBC molecules. This phenomenon illustrates the impact of linker rigidity on the field-dependent conformational change of dimesogen ChLCs.

The dependence on bias polarity of the STM imaging of a Ch-14 monolayer physisorbed on a highly oriented pyrolytic graphite (HOPG) surface is illustrated in Figure 1. Distinctively different stripe-patterned images can be observed for Ch-14 assemblies under negative and positive bias conditions (Figure 1a and c). The two-row brighter bands composed of Ch groups with alternately brighter and slightly dimmer structures are ascribed to the stereoscopic structure of the five- and six-membered rings in the Ch groups, and the darker bands in the image correspond to the flexible alkane chains linking the two cholesteric moieties. The medium-contrast image in the middle of the bright bands corresponds to the aligned isohexyl groups at both ends of the Ch-14 molecules. The proposed packing model for Ch-14 assembly indicates apparent dimer structures.

As a result of the stereoscopic structure of the Ch groups, these groups and the alkyl chains cannot be clearly resolved simultaneously in the same STM image because of their different height positions. By reducing the bias to a lower value, the orientation of the alkyl chain can be identified with a loss of Ch resolution (Figure 1b). The Ch-14 molecules are adsorbed with their alkyl chains oriented at a $(30 \pm 1)°$ angle to the axis of the bright band. The distances between the neighboring alkane chains (1.1 nm) are restricted by the width of the head groups. Note that the van der Waals interaction between the alkane chains in such an arrangement should be much weaker than that for the close-packed chains in assemblies of alkanes or alkane derivatives ((4.28 ± 0.02) Å for alkanes and (4.56 ± 0.05) Å for alkanols[7]). Therefore, the driving interactions for the assembly are considered to originate from the interaction between the cholesteric head groups. A schematic model of two Ch-14 molecules superimposed on the image of Figure 1b shows that the tilt angle of the two adjacent mesogen groups to the alkane chain is different, which would result in an asymmetric conformation with one Ch group higher than another, as demonstrated by the alternating contrast of Ch groups in Figure 1a.

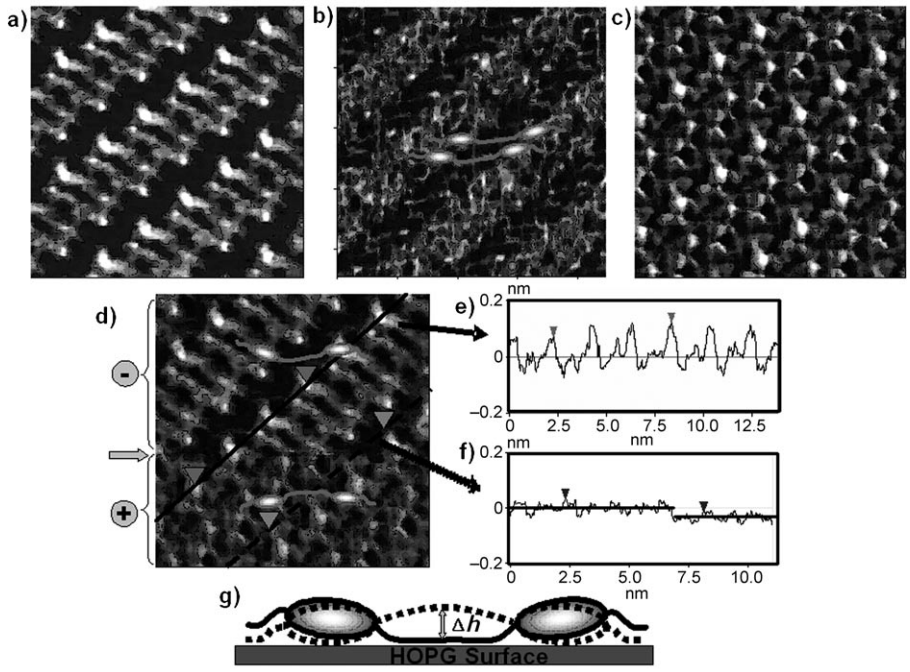

Figure 1. a) HR STM image of a SAM of Ch-14 molecules at negative bias (imaging conditions: 250 pA and −891 mV). b) The alkyl chain is resolved at low bias voltage (imaging conditions: 270 pA and −589 mV). A schematic model of two Ch-14 molecules is superimposed on the image. c) HR STM image of a SAM of Ch-14 molecules at positive bias (imaging conditions: 232 pA and 891 mV). d) HR STM image of Ch-14 molecular assembly structure at alternate bias polarities. The line where the bias change took place is marked by a gray arrow. For each section, the tunneling conditions are $|V_{bias}| = 890$ mV, $I_{set\ point} = 232$ pA; the choice of bias polarity is indicated by − or +. The image sizes for (a)–(d) are 11.2×11.2 nm^2. e, f) Cross-sectional profiles corresponding to the white solid line and the white dashed line in (d), respectively. The marked lines in (f) represent sections corresponding to positive (left) and negative (right) bias regions. g) Proposed model for the conformation change of the molecular chord. The solid line represents the side-view molecular structure at negative bias, and the dashed line represents the molecular structure at positive polarity. The height difference of alkane chains in the two conformations is shown as Δh.

When a positive sample bias was applied, the apparent contrast distribution of the stripe structure was transformed as indicated in the high-resolution (HR) STM image of the Ch-14 assembly (Figure 1c). This reversible image change is clearly shown in Figure 1d, in which the bias polarity was opposite for the upper (negative bias) and lower (positive bias) regions. The switching of bias voltage during scans generated only negligible disturbance to the STM image, mostly identified as a barely noticeable jump of scan line in the original STM image that can assist with the recognition of the position of bias switching. The difference between the two opposite bias voltages is about or less than 2 V, which is below the typical value of voltage pulses that can generate appreciable damage to the graphite surface,[8] and the feedback is kept active during such switching. Such instant contrast variation of Ch-14 that is changed by reversing the electric field direction can also be seen in the accompanying cross-sectional profiles in Figure 1e and f, which correspond to the white solid and dashed lines in Figure 1d, respectively. The

measured height of the alkane chains at negative bias is (0.05 ± 0.02) nm lower than that at the positive bias, while the measured height of the head groups at negative bias is nearly identical to that at the positive bias. Such bias-polarity-dependent contrast variation associated with alkane linking units in Ch-14 was reproducible in repeated experiments under different imaging conditions (see Supporting Information), and has never been reported for simple alkanes and alkane derivatives.

The same bias-dependent conformational changes can be observed at different imaging conditions, with higher contrast at positive bias and lower contrast at negative bias for alkane linking chains (see Supporting Information). The consistency in the contrast variation of the linking units is supportive of the results presented in Figure 1. Note that systematic variations can be identified in association with the cholesteric groups, as revealed by the sectional profiles at different tunneling conditions (see Figure 1e and the Supporting Information). Therefore, the contrast variations from the localized swaying of the mesogen parts schematically illustrated in Figure 1g could be considered insignificant. In addition, variations of mesogen parts among independent images could be attributed to different image conditions and different STM tips.

In the case of alkane derivatives, the vertical contrast in the STM image of the methylene regions is dominated by the hydrogen atom positions predicted by perturbation theory and extended Hückel calculations, and is therefore dominated by topography effects and does not have any discernible dependence on the magnitude and polarity of the bias voltage.[9–11] The variation in vertical contrast of the functional groups of various alkane derivatives relative to the methylene units was affected by both topographic and electronic factors, with ionization potential (IP) accounting for the observed contrast. A lower IP leads to higher contrast in the STM images. This correlation could originate from the contribution of the HOMO to the tunneling current in STM. A lower IP corresponds to closer energy levels between the HOMO and the Fermi level of the tip, and more diffuse molecular orbital structures. Both effects are beneficial to the enhancement of the coupling between the adsorbate and the tip.

It has been concluded that no dependence on bias polarity can be observed for either methylene units or terminal functional groups.[9–11] These studies are complementary to our observations, which show little observable dependence on bias polarity of the mesogen unit in both specimens examined, while the contrast variation is solely associated with the methylene portion. It is therefore reasonable to conclude that the contrast of the mesogen unit does not contribute to the observed contrast reversal of the methylene units.

A control STM experiment was conducted with alkanes and Ch-14 molecules in the same image (see Supporting Information). An apparent contrast variation for the C_{14} linking chains in Ch-14 molecules can be observed, while no observable contrast changes can be found for the alkane molecules. Therefore, the observed contrast variation of alkane linking units at alternate bias polarities can only be attributed to the positional variation, rather than the electronic structures of the HOMO and LUMO of the alkanes.

According to the above results and analysis, it is plausible to attribute the image contrast variations to the field-dependent bistable conformational change of the dimesogen ChLCs with flexible chains. The proposed conformational change induced by an electric field is illustrated in Figure 1g with a side view of the molecular structure. The long connecting lines stand for the C_{14} flexible linking chains and the spindle-shaped structures for the stereoscopic structure of Ch groups. The short tails attached to the spindles represent the isohexyl tails on the Ch groups. This scheme is a simplified description that ignores the asymmetric conformation observed in STM images.

It has been reported that large dipole moments exist in cholesteric molecules.[4] We calculated the charge populations of the Ch-14 molecules (see Supporting Information) and found that the linker alkane chains are almost neutrally charged, while the dipole moments are mainly contributed by the mesogen part (the dipole moment vectors of the mesogen part are presented in the Supporting Information). It is clear that the dominant dipole moment vector is along the y and z axes, that is, approximately perpendicular to the direction of the linking unit. As demonstrated in Figure 1g, when a negative bias is applied the alkyl chains tend to position themselves close to the graphite surface (illustrated as a solid-line structure). When the bias polarity was abruptly switched to positive, the dipoles of the Ch head group tend to rotate accordingly, which results in upward swinging of the flexible linking chains (illustrated as a dashed-line structure). The height difference of the alkane chains (Δh) is determined from the measured cross-sectional profile. The value of Δh measured from different images is (0.05 ± 0.02) nm (see Figure 1d and the Supporting Information). This molecular chord structure of the Ch-14 molecule can be switched between two bistable states using an electric field.

In a parallel study, large-scale assembly structures of CBC molecules containing a rigid linker unit can be observed on a HOPG surface. The assembly structure of CBC is also in the form of a stripe pattern, with bright bands composed of stereoscopic cholesteric moieties and relatively low-contrast bands corresponding to the rigid linking chains of biphenylene groups (Figure 2a). The contrast of the biphenyl groups is reduced in comparison with that of the Ch groups because of their lower topographical position. Identical structures and contrast of the CBC monolayer can be observed independent of bias polarities and bias values (Figure 2b), which is indicated in the sectional profiles in Figure 2c and d. No clear alternative arrangement of Ch groups was observed because of the flat conformation of biphenylene groups parallel to the HOPG surface. Different images for CBC assemblies at different locations using different tips were obtained for verification (see Supporting Information).

According to the packing model of CBC illustrated in Figure 2e, the isohexyl groups are aligned nearly perpendicular to the molecular axis. The two isohexyl groups show higher contrast as brighter dots located at both sides of Ch head groups. This observation is illustrative of the appreciable effects of linker units on the details of the assembling characteristics as a result of varied intermolecular interactions.

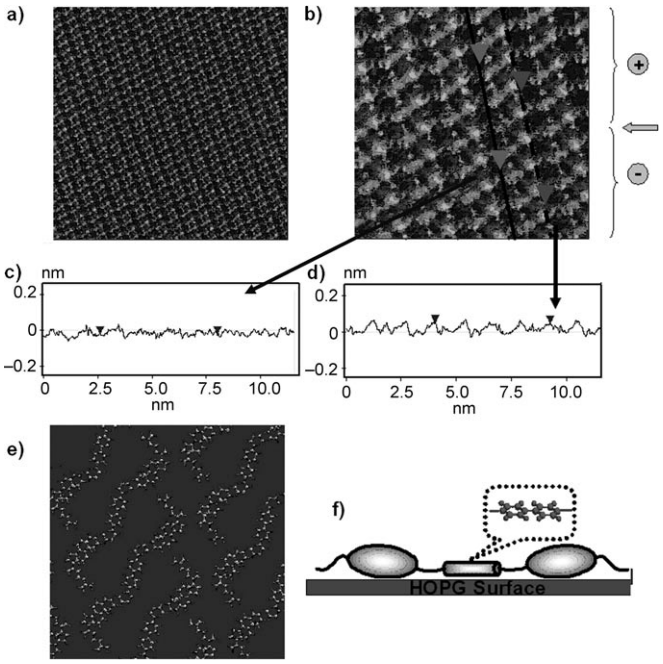

Figure 2. a) STM image (35.5×35.5 nm^2) of a CBC molecular assembly (imaging conditions: 300 pA and 700 mV). b) HR STM image (11.3×11.3 nm^2) of a CBC molecular assembly at both negative and positive bias polarities. The scan line where bias changes took place is marked by gray arrow. The tunneling conditions are 300 pA and 700 mV for the upper region and 300 pA and −950 mV for the lower region. The choice of bias polarity is indicated by − or +. c, d) Cross-sectional profiles corresponding to the white solid line and the white dashed line in (b), respectively. e) Proposed packing model of CBC molecules. f) Proposed side view of the molecular conformation of the CBC molecule. The rodlike feature in the middle represents the biphenylene group.

The proposed side view of the molecular conformation of the CBC molecule is shown in Figure 2 f. The spindle-shaped features and the short tails represent the Ch groups and the isohexyl tails, respectively. The rod in the middle represents the biphenylene group, which is illustrated as a flat configuration parallel to the graphite surface. As a result of the rigid biphenylene linker in CBC molecules, the electrically induced dipole rotation of the Ch groups is restricted with no observable conformational changes as shown for Ch-14 with flexible linking chains. Additionally, the π–π interaction between the graphite substrate and the biphenylene groups in CBC molecules may contribute partially to this restriction on conformational change.

In summary, two kinds of low-molecular-weight cholesterol dimesogens have been synthesized with a flexible alkyl chain (Ch-14) and a rigid biphenylene linker (CBC). The molecular assembly structures of Ch-14 and CBC were studied by STM. Conformational bistability was observed for Ch-14 molecules when the bias polarity was switched abruptly during imaging, while no discernible conformational changes were observed for the CBC molecules containing a rigid linking unit. This drastic difference in the conformational response of Ch-14 and CBC can be ascribed to the structural flexibility of Ch-14 with a flexible linker, while the response is restricted by the rigid biphenylene linker in CBC molecules. This in situ investigation of the field-dependent conformational bistability of ChLCs with a soft linker unit may lead to new design strategies for ChLC molecules, as well as functional molecular surfaces.

Experimental Section

Synthesis of Ch-14 (**2**): Ch-14 was synthesized by esterification of the commercially available tetradecanedioic acid (**1**) and cholesterol (Ch-OH) with DCC and 4-dimethylaminopyridine (DMAP) as described in the literature.[12,13] Ch-OH (15.47 g, 40 mmol), DCC (8.41 g, 40 mmol), and DMAP (0.49 g, 4 mmol) were dissolved in CH_2Cl_2 (70 mL), then **1** (5.16 g, 20 mmol) was added with stirring over 30 min. The mixture was stirred at room temperature for an additional 12 h. After removal of the precipitate by filtration, the solution was concentrated by rotary evaporation. The crude product was purified by column chromatography (silica gel) with hexane/ethyl acetate/acetic acid (10:1:1) as eluent to obtain pure Ch-14 as a white powder.

Synthesis of CBC (**4**): Ch-OH (3.867 g, 10 mmol), succinic anhydride (1.001 g, 10 mmol), and DMAP (0.122 g, 1 mmol) were dissolved in CH_2Cl_2 (100 mL), and the mixture was heated at reflux for 24 h. The solvent was removed by rotary evaporation, and the residual solid was recrystallized twice in glacial acetic acid to give cholesteryl hydrogen succinate (**3**) as a white powder. Compound **3** (0.973 g, 2 mmol), benzidine (0.184 g, 1 mmol), DMAP (0.0122 g, 0.1 mmol), and DCC (0.412 g, 2 mmol) were dissolved in CH_2Cl_2 (100 mL). The mixture was heated at reflux for 24 h and then cooled to room temperature. The solvent was removed by rotary evaporation, and the residual solid was washed three times with water. The crude product was further purified by column chromatography (silica gel) with CH_2Cl_2/petroleum ether (3:1) as eluent.

STM investigations: For preparation of the STM samples, the compounds were dissolved in toluene (HPLC grade) at a concentration of less than 1 mmol L^{-1}. The surface assembly of ChLC molecules was performed by depositing a droplet of the toluene solution directly onto a freshly cleaved graphite surface. The STM experiments were carried out with a Nanoscope IIIa system (Veeco Metrology Group, USA) at room temperature. Mechanically formed Pt/Ir (80:20) tips were used in the STM experiments. All images were recorded in the constant-current mode, and the specific tunneling conditions are given in the figure captions.

Computational details: Theoretical calculations were performed using density functional theory (DFT) provided by the DMol3 code.[14] The Perdew and Wang parameterization[15] of the local exchange-correlation energy was applied in the local spin density approximation (LSDA) to describe exchange and correlation. We expanded the all-electron spin-unrestricted Kohn–Sham wave functions in a local atomic orbital basis. In the double-numerical basis set, the valence s and p orbitals were represented by two basis functions each, and the d-type wave function on each atom was used to describe polarization. An angular momentum number one greater than the maximum angular momentum number in the atomic orbital basis was applied to specify the multipolar fitting that describes the analytical forms of the charge density and the Coulombic potential.[16] All calculations were all-electron and performed with the Extra-Fine mesh. The self-consistent field procedure was carried out with a convergence criterion of 10^{-5} a.u. on the energy and electron density.

Received: March 9, 2006
Revised: August 10, 2006
Published online: September 26, 2006

Keywords: dimesogens · liquid crystals · monolayers · scanning tunneling microscopy · single-molecule studies

[1] X. H. Qiu, G. V. Nazin, W. Ho, *Phys. Rev. Lett.* **2004**, *93*, 196806.
[2] J. Lahann, S. Mitragotri, T.-N. Tran, H. Kaido, J. Sundaram, I. S. Choi, S. Hoffer, G. A. Somorjai, R. Langer, *Science* **2003**, *299*, 371.
[3] V. A. Mallia, N. Tamaoki, *Chem. Soc. Rev.* **2004**, *33*, 76.
[4] N. Tamaoki, G. Kruk, H. Matsuda, *J. Mater. Chem.* **1999**, *9*, 2381.
[5] T. Ikeda, *J. Mater. Chem.* **2003**, *13*, 2037.
[6] N. Tamaoki, *Adv. Mater.* **2001**, *13*, 1135.
[7] K. Morishige, Y. Takami, Y. Yokota, *Phys. Rev. B* **1993**, *48*, 8277.
[8] T. R. Albrecht, M. M. Dovek, M. D. Kirk, C. A. Lang, C. F. Quate, D. P. E. Smith, *Appl. Phys. Lett.* **1989**, *55*, 1727.
[9] C. L. Claypool, F. Faglioni, A. J. Matzger, W. A. Goddard III, N. S. Lewis, *J. Phys. Chem. B* **1999**, *103*, 9690.
[10] C. L. Claypool, F. Faglioni, W. A. Goddard III, H. B. Gray, N. S. Lewis, R. A. Marcus, *J. Phys. Chem. B* **1997**, *101*, 5978.
[11] L. Giancarlo, D. Cyr, K. Muyskens, G. W. Flynn, *Langmuir* **1998**, *14*, 1465.
[12] G. Höfle, W. Steglich, H. Vorbrüggen, *Angew. Chem.* **1978**, *90*, 602; *Angew. Chem. Int. Ed. Engl.* **1978**, *17*, 569.
[13] A. Theis, H. Ritter, *Macromolecules* **2003**, *36*, 7552.
[14] A. Becke, *J. Chem. Phys.* **1988**, *88*, 2547.
[15] J. P. Perdew, Y. Wang, *Phys. Rev. B* **1992**, *45*, 13244.
[16] E. J. Baerends, D. E. Ellis, P. Ros, *Chem. Phys.* **1973**, *2*, 41.

